

Processor-in-the-loop performance validation of a three-phase NPC three-level inverter using a novel sinusoidal PWM technique for scalar control of an induction motor

Badr N'hili¹, Souhail Barakat¹, Abdelouahed Mesbahi¹, Mohamed Khafallah¹, Ayoub Nouaiti²

¹Department of Electrical Engineering, National High School of Electricity and Mechanics (ENSEM), Hassan II University of Casablanca, Casablanca, Morocco

²Laboratory of Spectrometry of Materials and Archeomaterials (LASMAR), Moulay Ismail University, Meknes, Morocco

Article Info

Article history:

Received Apr 25, 2025

Revised Oct 3, 2025

Accepted Oct 17, 2025

Keywords:

Multilevel inverter

Processor in the loop

Pulse width modulation

Scalar control

Total harmonic distortion

ABSTRACT

This paper presents the performance of a three-phase, three-level neutral point clamped inverter driving an induction motor for variable-speed applications, compared to a two-level inverter. The studied inverter operates using a novel sinusoidal pulse width modulation technique that improves the quality of voltage and current output signals while increasing efficiency. Motor speed control is achieved using the scalar control (V/Hz) method. Experimental validation of the simulation results is performed by executing the generated C code on the F28379D DSP LaunchPad within the MATLAB/Simulink and Code Composer Studio environment, applying the processor-in-the-loop (PIL) technique.

This is an open access article under the [CC BY-SA](#) license.



Corresponding Author:

Badr N'hili

Department of Electrical Engineering, National High School of Electricity and Mechanics (ENSEM)

Hassan II University of Casablanca

Casablanca, Morocco

Email: badr.nhili@ensem.ac.ma

1. INTRODUCTION

Multilevel inverters (MLI) are a type of DC-AC converter that generates output voltage with multiple voltage levels. They have a wide range of applications, particularly in the conversion of energy stored in batteries or sourced from renewable energy systems, such as solar panels and wind turbines. Advances in power electronics and semiconductor technology have increased the efficiency of these electrical systems [1]-[5]. Notably, multilevel inverters enhance the quality of generated signals and reduce the size of filters and the number of switches [6]-[10]. The various topologies of multilevel inverters are the cascaded H-bridge, the flying capacitor (FC), and the neutral point clamping (NPC) configurations [11]-[17].

In this work, a novel pulse width modulation technique that significantly enhances the quality of the transmitted power is used to control an induction motor via a three-phase, three-level neutral point clamped inverter (3-P 3-L NPC inverter) widely used in variable speed drives and excels in reducing harmonic distortion in output current and voltage. The motor's speed control is then achieved by applying the scalar control method. The validation of the results is conducted using the processor-in-the-loop (PIL) technique within the MATLAB/Simulink environment and the DSP LaunchPad from the C2000™ family of microcontrollers.

2. THE PROPOSED ALGORITHM

Various pulse width modulation (PWM) techniques, including multi-carrier sinusoidal PWM, space vector PWM, and selective harmonic elimination, are widely employed for controlling multilevel inverters and regulating the AC output of power electronic converters [18]-[23]. These techniques enable the generation of optimized switching patterns that yield an output current waveform closely approximating a sinusoidal signal.

In this work, a novel modulation strategy is applied to a three-phase, three-level neutral-point-clamped (NPC) inverter within a DSP-based control environment. The proposed sinusoidal PWM method extends the approach originally introduced by Rahim and Selvaraj [24] and N'hili *et al.* [25], by incorporating an adaptation that simplifies the generation of gating signals for the power switches of the 3P-3L NPC inverter. This adaptation not only facilitates efficient modulation index control but also enhances harmonic distortion performance. The proposed method operates by comparing a high-frequency triangular carrier signal, V_c , with two low-frequency sinusoidal reference signals, V_{ref1} and V_{ref2} . The second reference signal, V_{ref2} , is phase-aligned with V_{ref1} but shifted by a DC offset equal to the amplitude of V_c (Figure 1).

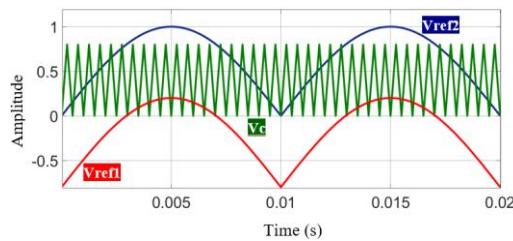


Figure 1. Carrier (V_c) and reference (V_{ref1} , V_{ref2}) signals generated for the sinusoidal PWM technique presented by Rahim and Selvaraj [24]

Compared with the original technique, which was developed for a single-phase multistring five-level inverter, the proposed SPWM method does not require rectification of the reference signals. The comparison process starts with V_{ref1} and proceeds until it reaches zero, after which V_{ref2} assumes control until it exceeds the carrier's peak amplitude V_c (Figure 2, see Appendix). The control strategy for each arm consists of applying to T4 (U, V, W) the same control signal as T1(U, V, W) with a phase shift by $\pi/2$. Meanwhile, T3 (U, V, W) and T2 (U, V, W) receive the inverse of the control signals applied to T1 (U, V, W) and T4 (U, V, W), respectively, as defined in (1)-(3).

$$T4(U, V, W) = T1(U, V, W) + \pi/2 \quad (1)$$

$$T3(U, V, W) = \overline{T1(U, V, W)} \quad (2)$$

$$T2(U, V, W) = \overline{T4(U, V, W)} \quad (3)$$

The modulation index (MI) in this case is obtained using (4). The amplitude of the carrier signal is represented by V_c , and the amplitude of the reference signal is represented by V_{ref} . In order to get a signal with lower harmonic content, the modulation index value must be between 0.5 and 1.

$$MI = \frac{V_{ref}}{V_c} \quad (4)$$

3. METHOD

3.1. System description

The proposed 3-P, 3-L inverter has the NPC topology as a configuration. The power circuit of the inverter is depicted in Figure 3. The proper control of the switches allows the inverter to produce three output voltage levels: 0, $+E/2$, and $-E/2$.

3.2. System operation

During the operation of the system, the value of the voltage V_{AO} between the terminal A of the load and the neutral point O depends on the conducting or blocking states of the four switches T1u, T2u, T3u, and T4u of the arm U. The three configurations of {T1u, T2u, T3u, T4u} are {1100}, {0110} and {0011} as shown in Figure 4. The switching states of the power switches and the corresponding synthesized output voltages are summarized in Table 1.

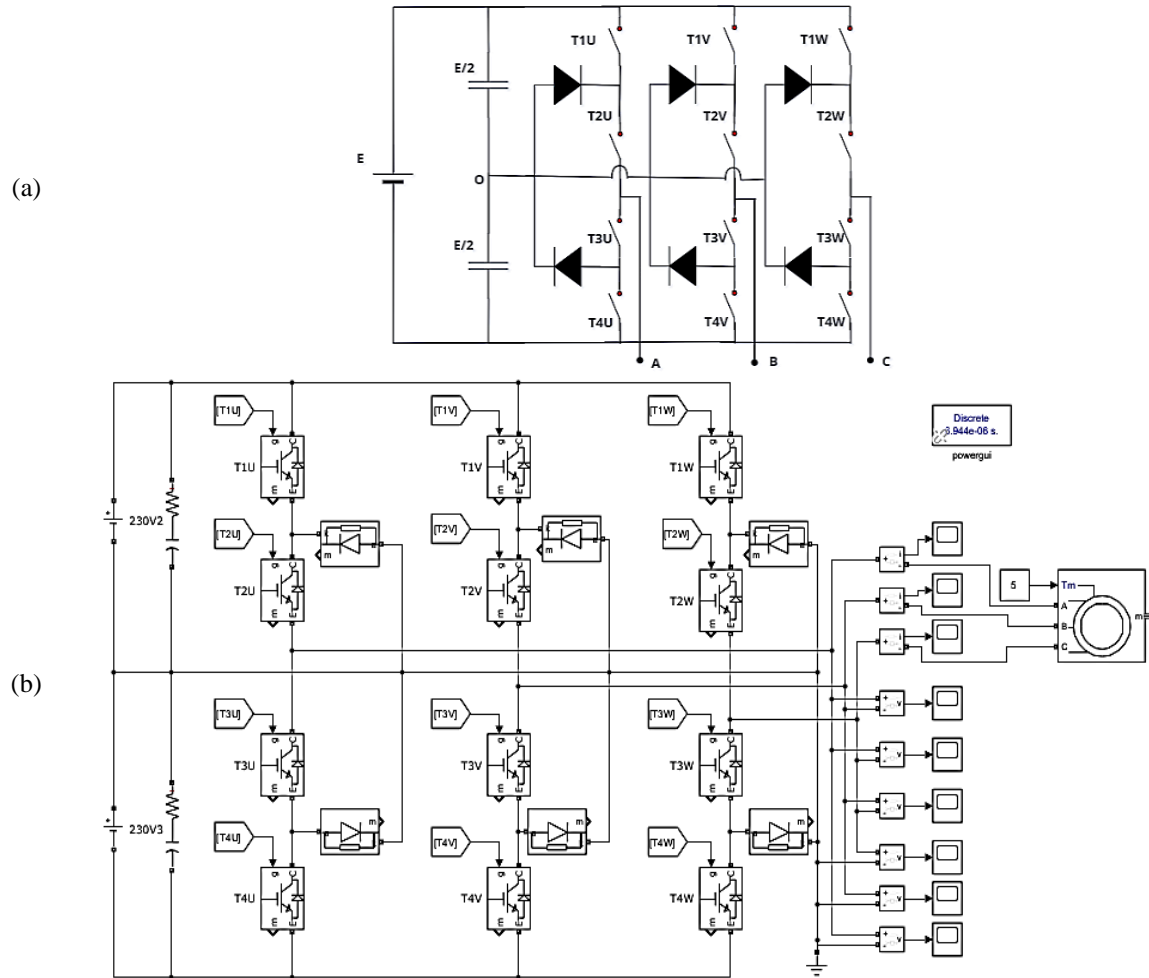


Figure 3. Configuration of the proposed MLI: (a) scheme of the proposed 3-P 3-L NPC inverter and (b) MATLAB/Simulink scheme of the proposed inverter associated with the induction motor

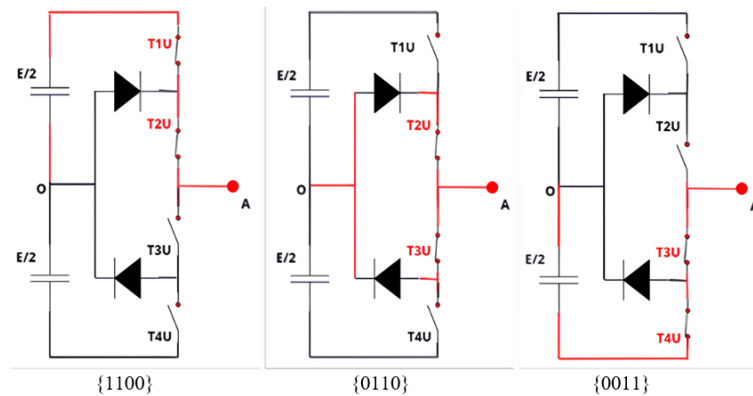


Figure 4. Operation of the proposed 3-P 3-L NPC inverter

Table 1. Switching states and the synthesized output voltages in the phase leg A

Switching states				Output voltages
T1U	T2U	T3U	T4U	
ON	ON	OFF	OFF	$+E/2$
OFF	ON	ON	OFF	0
OFF	OFF	ON	ON	$-E/2$

4. RESULTS AND DISCUSSION

In this section, simulation results obtained using MATLAB/Simulink and the DSP environment (F28379D LaunchPad) are presented to compare the performance in terms of output signal quality. The comparison is carried out in Simulink using PWM generator blocks to control a three-phase two-level inverter, and both the multicarrier SPWM and the proposed modulation technique to control the three-phase three-level NPC inverter, operated through Simulink and the DSP card.

As a load, a squirrel-cage induction motor is employed, since such machines are widely used in variable-speed drives due to their cost-effectiveness, robustness, and reliability [26]. Both the 3P–2L inverter and the proposed 3P–3L NPC inverter are tested under a load torque of 5 N.m, with motor and inverters operating parameters given respectively in Tables 2 and 3. The comparative study includes spectral analysis of the output signals using MATLAB Simulink's fast fourier transform (FFT) function.

Table 2. Parameters of the induction motor

Parameters	Values
Nominal power P _n (VA)	1500
Voltage (line to line) V _n (Vrms)	400
Frequency (Hz)	50
Stator resistance R _s (ohm) and inductance L _{ls} (H)	[5.63 0.018]
Rotor resistance R _r ' (ohm) and inductance L _{lr} ' (H)	[2.89 0.018]
Mutual inductance L _m (H)	0.367

Table 3. Inverters' operating parameters

Parameters	Values
DC input voltage (E)	460 V
Carrier switching frequency	6 kHz
Reference frequency	50 Hz
Modulation Index	0.95

4.1. FFT Analysis of the 3-phase 2-level inverter output signals

The FFT analysis of the output voltage and current signals of the three-phase two-level inverter driving the induction motor under the conditions specified in Table 2 and 3, reveals a limited output voltage and poor signal quality, as indicated by the recorded total harmonic distortion (THD) values of 28.82% for the output line voltage and 27.31% for the load current (Figure 5). The speed achieved is approximately 1433 rpm, and the electromagnetic torque ranges between 4.2 and 6.3 N.m. (Figure 6).

4.2. Performance of the NPC 3-level inverter using the multi-carrier SPWM

The control of the induction motor using the 3-P 3-L NPC inverter and the conventionnel Sinusoidal PWM modulation technique, under the same conditions (Table 2 and 3), allowed us to observe the quality of the generated signals. The resulting PWM signals for the switch control are presented in Figure 7. The FFT analysis of the output signals shows a significant improvement in the quality of the signals, as indicated by the recorded harmonic distortion rates, less than 2% for both the output line voltage and the load current (Figure 8). The speed achieved is approximately 1435 rpm, and the electromagnetic torque ranges between 4.7 and 5.7 N.m (Figure 9).

4.3. Performance of the NPC 3-level inverter using the proposed PWM technique

The proposed sinusoidal PWM modulation technique is a new approach for Sinusoidal PWM, which allows an efficient adaptation to the considered DSP environment while enhancing the quality of the output signals. The proposed sinusoidal PWM technique (Figure 2) is used to generate the switching pattern (Figure 10) in order to control the 3-P 3-L, under the same conditions (Table 2 and 3).

As indicated by the recorded harmonic distortion rates obtained using the FFT analysis, the quality of the output signals was enhanced. In fact, the THD is less than 1.1% for both the output line voltage and the load current (Figure 11). The speed achieved is approximately 1435 rpm, and the electromagnetic torque ranges between 4.96 and 5.43 N.m (Figure 12). The obtained results demonstrate, on the one hand, that the performance of the three-phase three-level NPC inverter, in terms of output signal quality, harmonic distortion, and torque ripple, is superior to that of the conventional three-phase two-level inverter. On the other hand, controlling the inverter using the proposed modulation technique further enhances these performance metrics compared to conventional SPWM. Table 4 provides a summary of the obtained results.

Table 4. Performances of the 3-P 2-L inverter and the studied 3-P 3-L NPC inverter

Inverter/ modulation technique	Output current THD	Output line voltage THD	Torque ripple	Rotor speed (rpm)
3-P 2-L inverter/SPWM	27.31 %	28.82 %	42 %	1433
3-P 3-L NPC inverter/multi-carrier SPWM	1.78 %	1.40 %	19.76%	1435
3-P 3-L NPC inverter/proposed PWM technique	0.96 %	1.06 %	9.4 %	1435

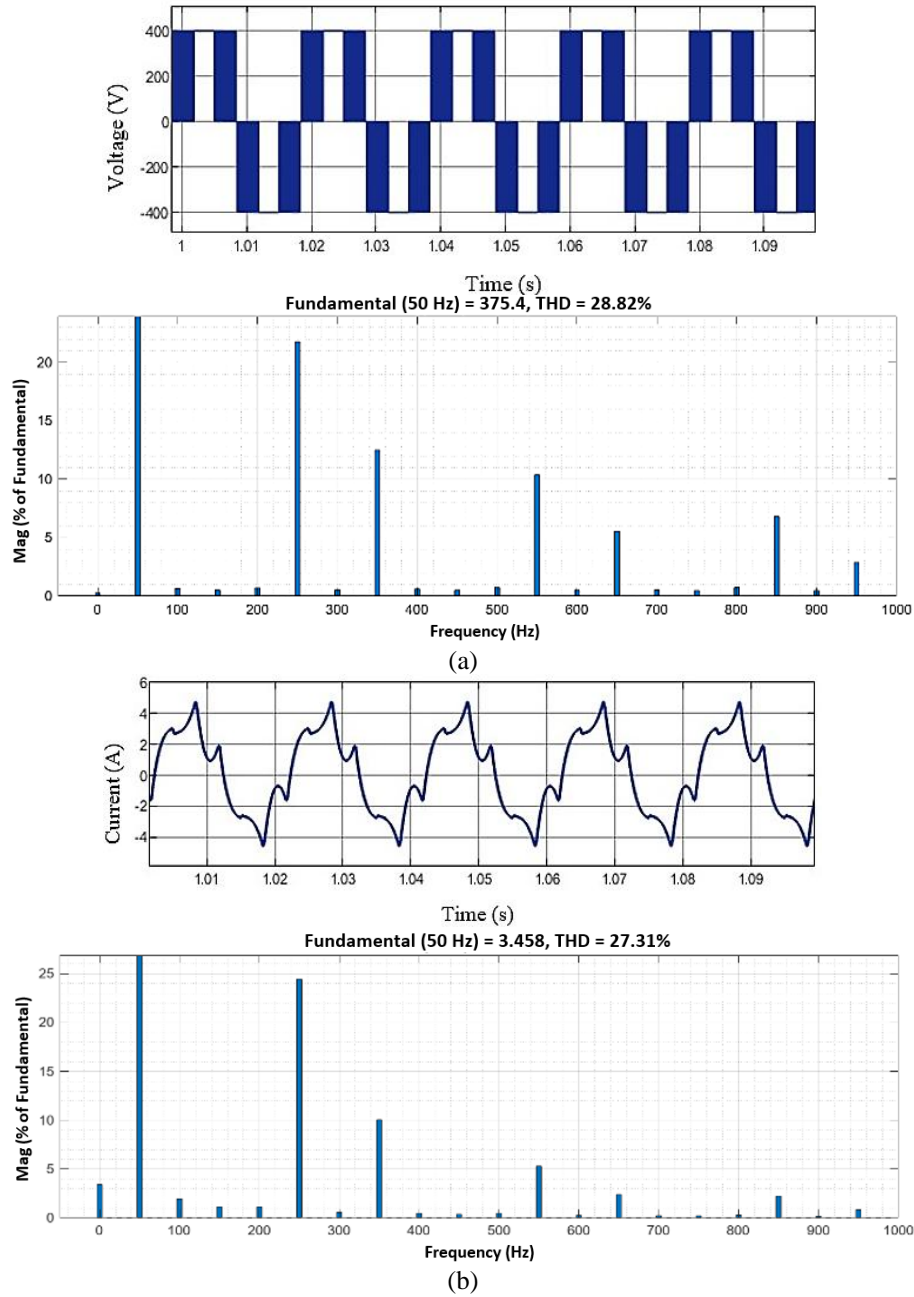


Figure 5. Voltage and current output signals of 3-P 2-L level inverter and FFT analysis: (a) line voltage U_{AB} and (b) current I_A

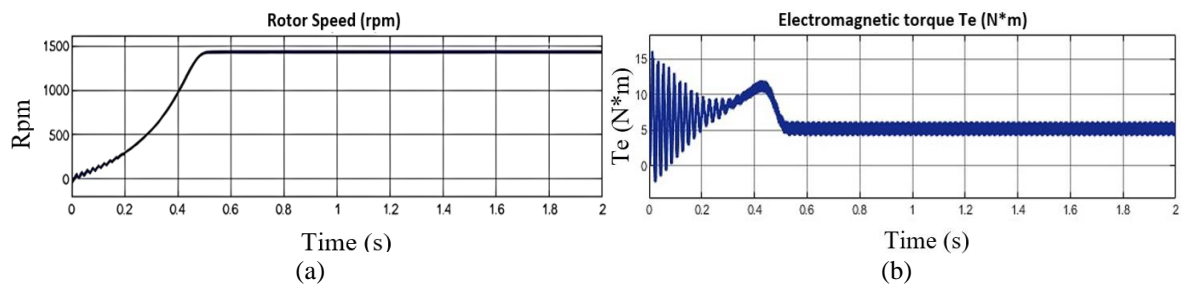


Figure 6. Speed curve and electromagnetic torque responses of the induction motor using the 3-P 2-L inverter: (a) rotor speed rpm and (b) electromagnetic torque T_e

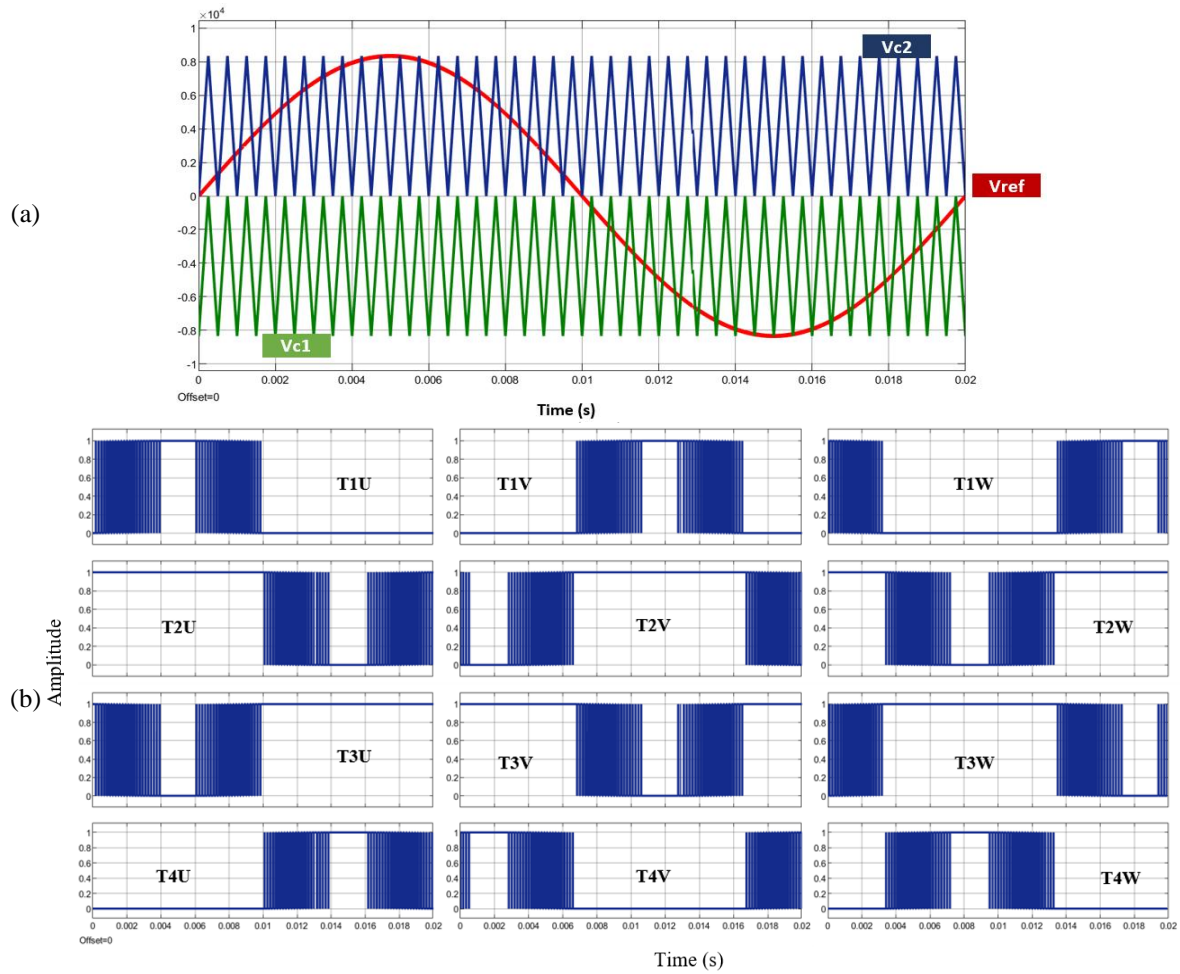


Figure 7. Multi-carrier SPWM technique for the 3-P 3-L NPC: (a) carrier and reference signals used for the switching pattern generation, and (b) PWM switching scheme of U, V and W phase legs

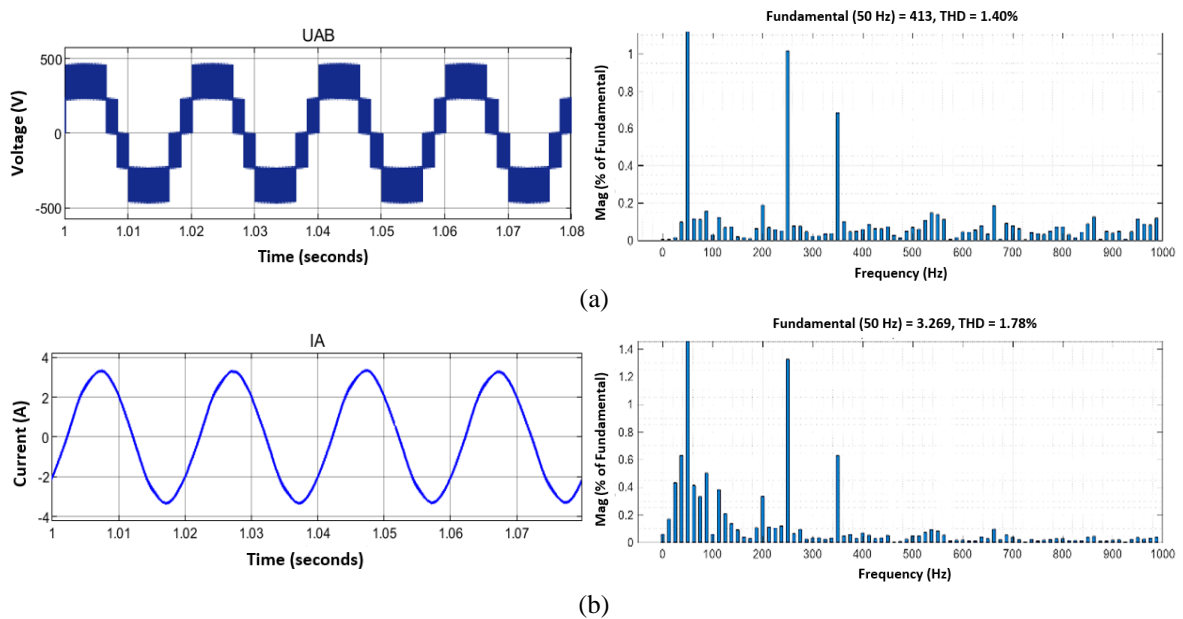


Figure 8. Voltage and current output signals of the studied 3-P 3-L level NPC inverter and FFT analysis: (a) line voltage U_{AB} and (b) current I_A

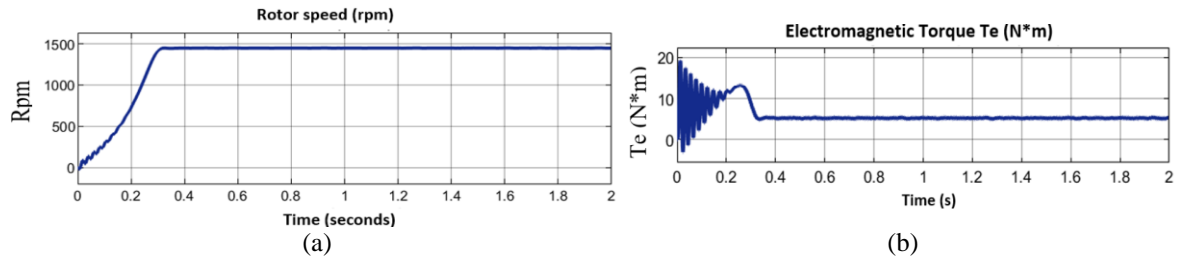


Figure 9. Speed curve and electromagnetic torque responses of the induction motor using the studied 3-P 3-L NPC inverter: (a) rotor speed rpm and (b) electromagnetic torque T_e

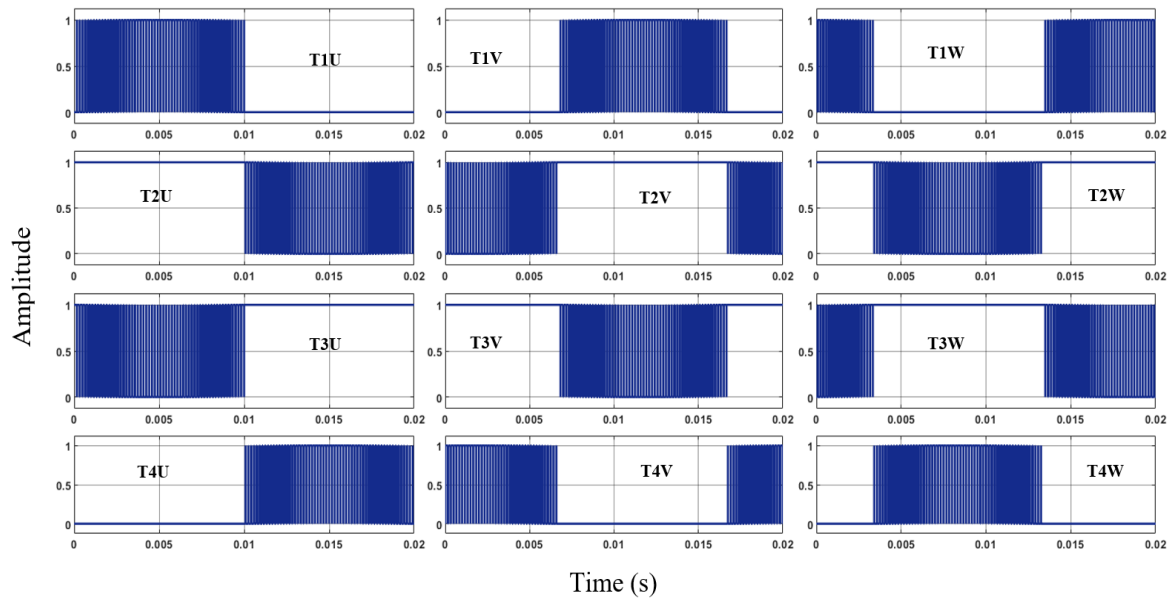


Figure 10. Proposed PWM switching scheme of U, V and W phase legs

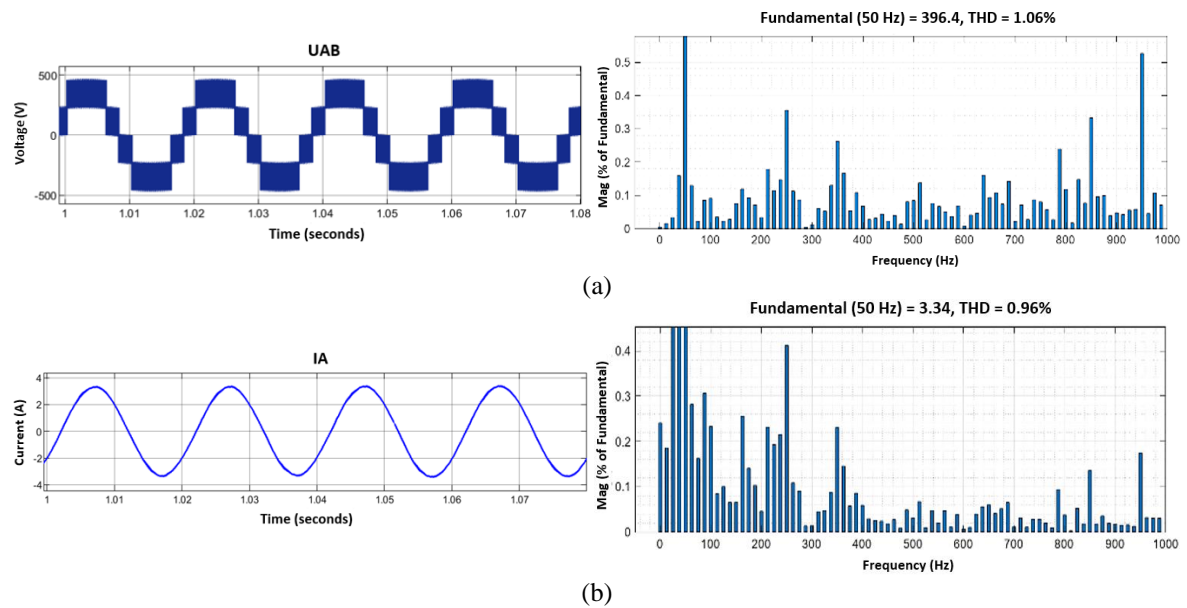


Figure 11. Voltage and current output signals of the studied 3-P 3-L level NPC inverter and FFT analysis: (a) line voltage U_{AB} and (b) current I_A

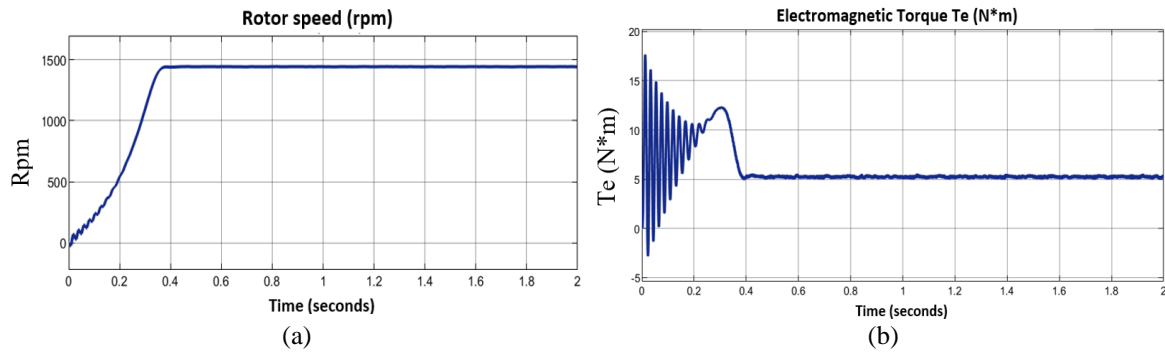


Figure 12. Speed curve and electromagnetic torque responses of the induction motor using the studied 3-P 3-L NPC inverter: (a) rotor speed rpm and (b) electromagnetic torque T_e

4.4. Scalar control of the induction motor and PIL implementation

In this section, a scalar control is applied to the induction motor using the proposed modulation technique and the 3-P 3-L NPC inverter. This technique consists of maintaining a constant (voltage/frequency) ratio, corresponding to the nominal flux, throughout the full operating speed range. It is used for moderate precision applications and allows for reducing hardware investment costs [27].

The control algorithm designed on MATLAB/Simulink for the scalar control of the induction motor using the proposed Sinusoidal PWM technique is configured and adapted to ensure compatibility with the F28379D DSP launch pad development board (Figure 13) whose parameters are displayed in Table 5. The control algorithm is then validated using the processor-in-the-loop (PIL) technique. To create the Simulink PIL block, a C code, based on the developed scalar control algorithm and the proposed modulation technique, is generated using MATLAB/Simulink embedded coder, then loaded onto the development board as shown in Figure 14. During the simulation, Simulink communicates with the DSP in real time, such that the control computations are performed on the actual processor while the rest of the model runs on the host computer.

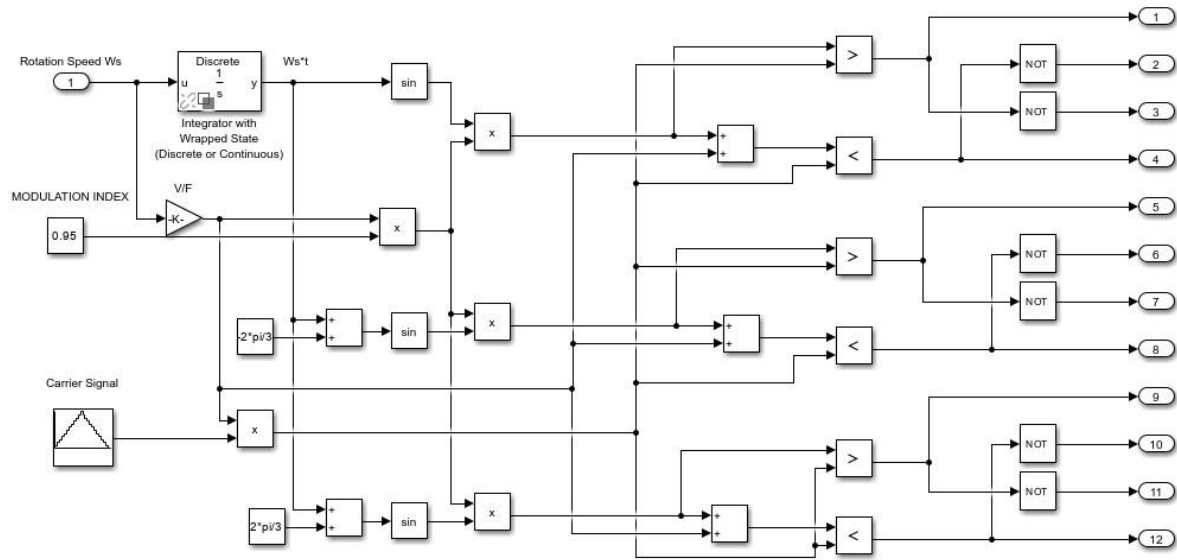
The spectral analysis of the synthesized inverter output line voltage and current waveforms, using the FFT tool of Simulink, is performed under the operating condition of $MI = 0.95$ with the variation of the motor speed using the PIL block of the proposed scalar control technique. The obtained results shown in Figure 15 demonstrate the efficiency of the proposed scalar control technique, allowing for enhancing the quality of the transmitted power, where THD rates around 1% are achieved for both output voltage and load current, during the variation in motor speed for frequencies of 35, 50, and 65 Hz. In addition, the load currents are displayed as nearly sinusoidal waveforms. The speed curve closely matches the setpoint, and the electromagnetic torque ranges between 4.8 and 5.4 N.m (Figure 16). Thus, the use of the proposed PWM technique in combination with the scalar control method has made it possible to leverage the advantages of this method in terms of simplicity, ease of implementation, and efficiency while improving the quality of the output signals (performance results in Table 6).



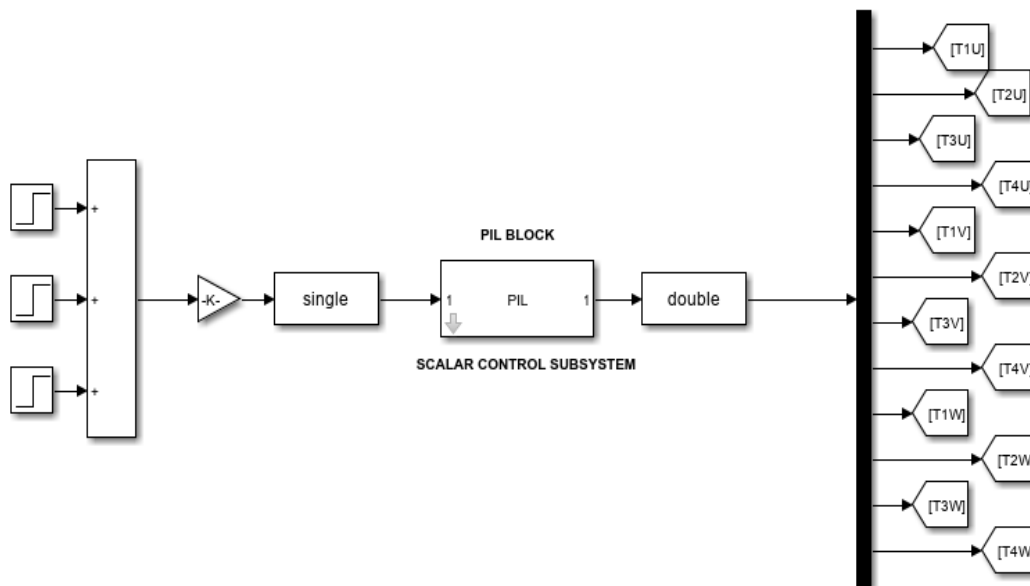
Figure 13. F28379D DSP launch pad

Table 5. Parameters of the DSP launch pad

Parameters	Values
Microcontroller	TMS320F28379D
Processor core	Dual C28x CPUs (200 MHz each)
Co-processor	Control law accelerator (CLA)
Memory	1 MB Flash, 204 KB RAM
Operating voltage	3.3 V (I/O), 5 V (supply via USB)



(a)

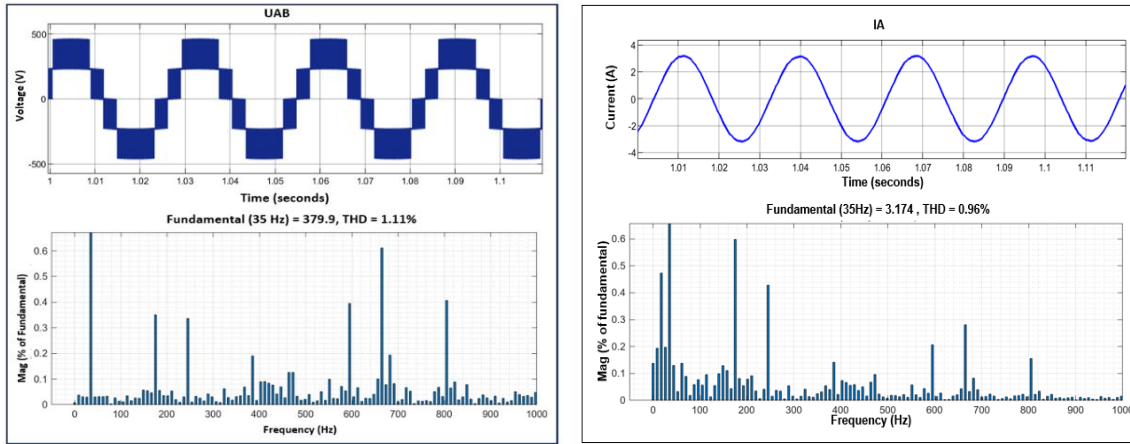


(b)

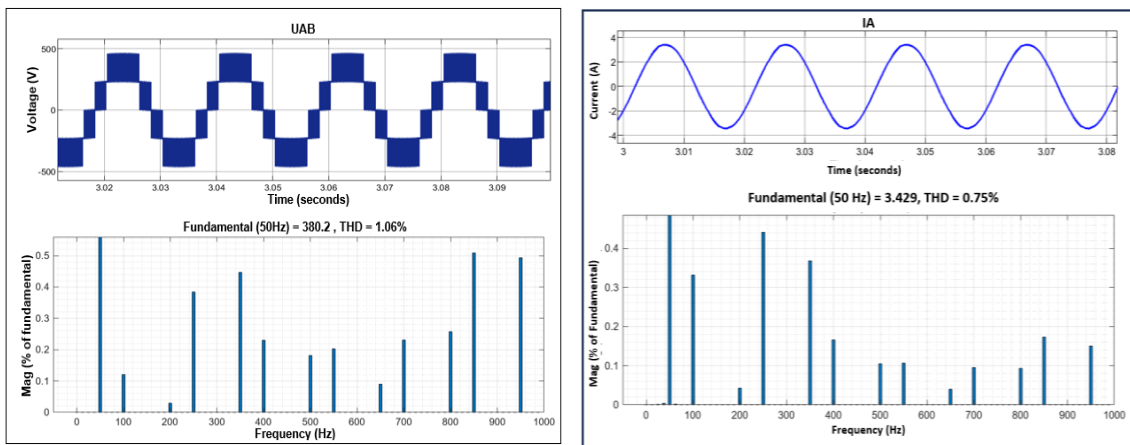
Figure 14. PIL block of the proposed scalar control generation:
 (a) proposed control algorithm and (b) generated PIL block

Table 6. Performance of the 3-P 3-L NPC inverter using PIL block of the proposed scalar control method

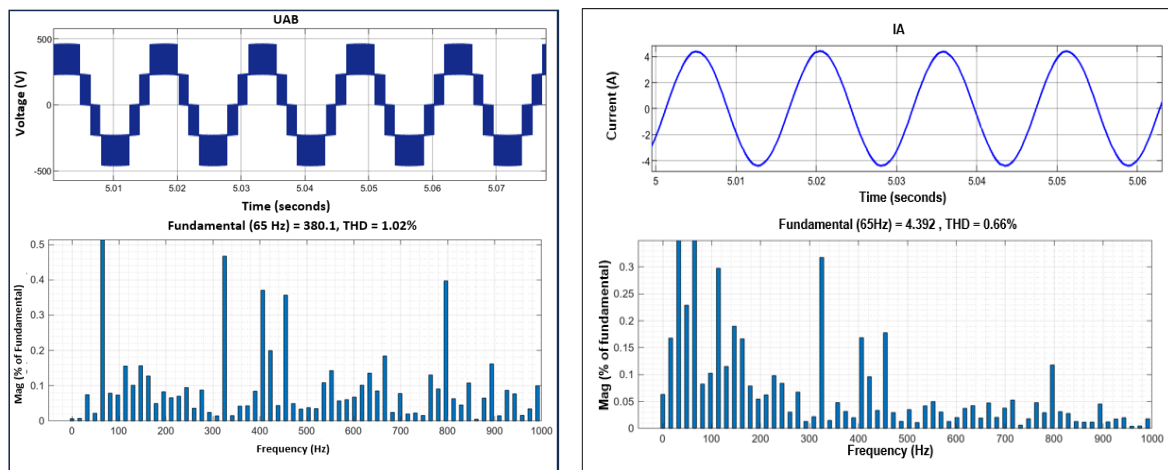
Set of motor speed frequency (Hz)	Output current THD	Output line voltage THD	Torque ripple	Rotor speed (rpm)
35 Hz	0.96%	1.11%	12%	1021
50 Hz	0.75%	1.06%	7%	1435
65 Hz	0.66%	1.02%	6.8%	1825



(a)



(b)



(c)

Figure 15. FFT analysis of output voltage and load current of the 3-P 3-L NPC inverter for different values of frequency (F) using the developed PIL block for the scalar control of the induction motor:

(a) $F = 35$ Hz, (b) $F = 50$ Hz, and (c) $F = 65$ Hz

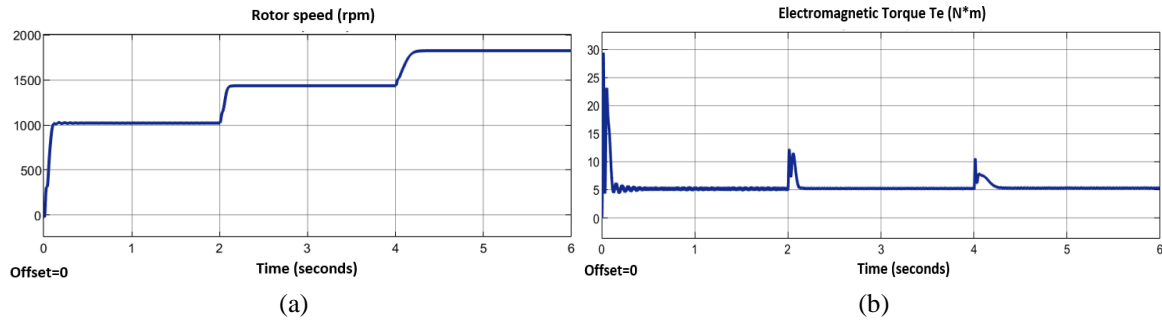


Figure 16. Speed curve and electromagnetic torque obtained using the PIL block for the scalar control of the induction motor through the staged 3-P 3-L NPC inverter: (a) rotor speed rpm and (b) electromagnetic torque T_e

5. CONCLUSION

This paper presents a novel PWM control technique for generating the switching signals to control a three-phase, three-level NPC inverter within a DSP environment. The inverter's circuit topology and operating principles are thoroughly analyzed. The performance of the proposed inverter is validated through simulation and experimental testing using the suggested sinusoidal PWM technique for scalar control of an induction motor.

Simulation results and PIL validation show that the proposed modulation technique, applied to the studied inverter, under nominal conditions, allows for achieving a THD less than 1% for both voltage and current output signals. Furthermore, the three-phase, three-level NPC inverter not only outperforms the three-phase, two-level inverter and the conventional SPWM technique of the three-phase, three-level NPC inverter, by achieving lower THD, but also enables simpler control implementation and efficient operation with improved performance. The data supporting the findings of this study are available within the article. The next steps involve applying other control strategies, including neural and genetic control.

FUNDING INFORMATION

The authors declare that this research received no specific grant from any funding agency in the public, commercial, or not-for-profit sectors.

AUTHOR CONTRIBUTIONS STATEMENT

This journal uses the Contributor Roles Taxonomy (CRediT) to recognize individual author contributions, reduce authorship disputes, and facilitate collaboration.

Name of Author	C	M	So	Va	Fo	I	R	D	O	E	Vi	Su	P	Fu
Badr N'hili	✓	✓	✓	✓	✓	✓	✓	✓	✓	✓	✓		✓	✓
Souhail Barakat	✓	✓				✓	✓	✓		✓	✓			
Abdelouahed Mesbahi	✓	✓	✓	✓	✓	✓	✓			✓	✓	✓	✓	✓
Mohamed Khafallah		✓				✓	✓			✓		✓	✓	
Ayoub Nouaiti		✓				✓	✓			✓				

C : **C**onceptualization

M : **M**ethodology

So : **S**oftware

Va : **V**alidation

Fo : **F**ormal analysis

I : **I**nterpretation

R : **R**esources

D : **D**ata Curation

O : **O**riginal Draft

E : **E**diting

Vi : **V**isualization

Su : **S**upervision

P : **P**roject administration

Fu : **F**unding acquisition

CONFLICT OF INTEREST STATEMENT

The authors declare that they have no known competing financial interests or personal relationships that could have influenced the work reported in this paper.

DATA AVAILABILITY

The data that support the findings of this study are available from the corresponding author, [BN], upon reasonable request.

REFERENCES

- [1] X. Lyu, J. Zhao, Y. Jia, Z. Xu, and K. Po Wong, "Coordinated control strategies of PMSG-based wind turbine for smoothing power fluctuations," *IEEE Transactions on Power Systems*, vol. 34, no. 1, pp. 391–401, Jan. 2019, doi: 10.1109/TPWRS.2018.2866629.
- [2] Y. Errami, A. Obbadi, S. Sahnoun, M. Ouassaid, and M. Maaroufi, "Hybrid control of wind energy conversion system based PMSG and three level NPC Converter," in *2019 7th International Renewable and Sustainable Energy Conference (IRSEC)*, IEEE, Nov. 2019, pp. 1–8. doi: 10.1109/IRSEC48032.2019.9078206.
- [3] T. Qanbari and B. Tousi, "Single-source three-phase multilevel inverter assembled by three-phase two-level inverter and two single-phase cascaded h-bridge inverters," *IEEE Transactions on Power Electronics*, vol. 36, no. 5, pp. 5204–5212, May 2021, doi: 10.1109/TPEL.2020.3029870.
- [4] H. Lin, M. Mehrabankhomartash, F. Yang, M. Saeedifard, J. Yang, and Z. Shu, "A flexible space vector modulation scheme for cascaded h-bridge multilevel inverters under failure conditions," *IEEE Transactions on Industrial Electronics*, vol. 69, no. 12, pp. 11856–11867, Dec. 2022, doi: 10.1109/TIE.2021.3128888.
- [5] A. Lewicki, I. C. Odeh, and M. Morawiec, "Space vector pulsewidth modulation strategy for multilevel cascaded h-bridge inverter with DC-link voltage balancing ability," *IEEE Transactions on Industrial Electronics*, vol. 70, no. 2, pp. 1161–1170, Feb. 2023, doi: 10.1109/TIE.2022.3158005.
- [6] M. D. Siddique, S. Mekhilef, N. M. Shah, J. S. M. Ali, and F. Blaabjerg, "A new switched capacitor 7l inverter with triple voltage gain and low voltage stress," *IEEE Transactions on Circuits and Systems II: Express Briefs*, vol. 67, no. 7, pp. 1294–1298, Jul. 2020, doi: 10.1109/TCSII.2019.2932480.
- [7] J. Rodriguez *et al.*, "Multilevel Converters: An enabling technology for high-power applications," *Proceedings of the IEEE*, vol. 97, no. 11, pp. 1786–1817, Nov. 2009, doi: 10.1109/JPROC.2009.2030235.
- [8] P. T. Giang, V. T. Ha, and V. H. Phuong, "Drive control of a permanent magnet synchronous motor fed by a multi-level inverter for electric vehicle application," *Engineering, Technology & Applied Science Research*, vol. 12, no. 3, pp. 8658–8666, Jun. 2022, doi: 10.48084/etasr.4935.
- [9] L. Vijayaraja, S. G. Kumar, M. Rivera, and E. Babaei, "Performance enhancement of reduced component multilevel inverter with optimal placement of level shifter," *IEEE Latin America Transactions*, vol. 22, no. 6, pp. 502–511, Jun. 2024, doi: 10.1109/TLA.2024.10534310.
- [10] W. Boucheriette, A. Moussi, R. Mechgoug, and H. Benguesmia, "A multilevel inverter for grid-connected photovoltaic systems optimized by genetic algorithm," *Engineering, Technology & Applied Science Research*, vol. 13, no. 2, pp. 10249–10254, Apr. 2023, doi: 10.48084/etasr.5558.
- [11] M. Malinowski, K. Gopakumar, J. Rodriguez, and M. A. Pérez, "A survey on cascaded multilevel inverters," *IEEE Transactions on Industrial Electronics*, vol. 57, no. 7, pp. 2197–2206, Jul. 2010, doi: 10.1109/TIE.2009.2030767.
- [12] K. Gudipati, H. V. R. Maramreddy, S. G. Kolli, V. Anantha Lakshmi, and G. Sreenivasa Reddy, "Comparison of pulse width modulation techniques for diode-clamped and cascaded multilevel inverters," *Engineering, Technology & Applied Science Research*, vol. 13, no. 4, pp. 11078–11084, Aug. 2023, doi: 10.48084/etasr.5939.
- [13] J. Huang and K. A. Corzine, "Extended operation of flying capacitor multilevel inverters," *IEEE Transactions on Power Electronics*, vol. 21, no. 1, pp. 140–147, Jan. 2006, doi: 10.1109/TPEL.2005.861108.
- [14] A. K. Sadigh, S. H. Hosseini, M. Sabahi, and G. B. Gharehpetian, "Double flying capacitor multicell converter based on modified phase-shifted pulsewidth modulation," *IEEE Transactions on Power Electronics*, vol. 25, no. 6, pp. 1517–1526, Jun. 2010, doi: 10.1109/TPEL.2009.2039147.
- [15] J. Rodriguez, S. Bernet, P. K. Steimer, and I. E. Lizama, "A survey on neutral-point-clamped inverters," *IEEE Transactions on Industrial Electronics*, vol. 57, no. 7, pp. 2219–2230, Jul. 2010, doi: 10.1109/TIE.2009.2032430.
- [16] R. Portillo, S. Vazquez, J. I. Leon, M. M. Prats, and L. G. Franquelo, "Model based adaptive direct power control for three-level NPC converters," *IEEE Transactions on Industrial Informatics*, vol. 9, no. 2, pp. 1148–1157, May 2013, doi: 10.1109/TII.2012.2209667.
- [17] M. K. Sahu, A. K. Panda, and B. P. Panigrahi, "Direct torque control for three-level neutral point clamped inverter-fed induction motor drive," *Engineering, Technology & Applied Science Research*, vol. 2, no. 2, pp. 201–208, Apr. 2012, doi: 10.48084/etasr.117.
- [18] Q.-T. Tran, "Control of grid-connected inverter using carrier modulation," *Engineering, Technology & Applied Science Research*, vol. 14, no. 4, pp. 15422–15428, Aug. 2024, doi: 10.48084/etasr.7789.
- [19] L. M. Grzesiak, B. Ufnalski, and A. Kaszewski, "An efficient discontinuous pulse width modulation algorithm for multilevel voltage-source converters," in *2011 IEEE International Symposium on Industrial Electronics*, IEEE, Jun. 2011, pp. 131–135. doi: 10.1109/ISIE.2011.5984145.
- [20] M. Karpanen, M. Hankaniemi, T. Suntio, and M. Sippola, "Dynamical characterization of peak-current-mode-controlled buck converter with output-current feedforward," *IEEE Transactions on Power Electronics*, vol. 22, no. 2, pp. 444–451, Mar. 2007, doi: 10.1109/TPEL.2006.889921.
- [21] P. N. Enjeti and S. A. Choudhury, "A new control strategy to improve the performance of a PWM AC to DC converter under unbalanced operating conditions," *IEEE Transactions on Power Electronics*, vol. 8, no. 4, pp. 493–500, Oct. 1993, doi: 10.1109/63.261020.
- [22] A. Nouaiti, A. Saad, A. Mesbahi, and M. Khafallah, "Implementation of A Single Phase Switched-Capacitor Nine-Level Inverter for PV system applications with selective harmonic elimination," *International Journal of Computer Applications*, vol. 168, no. 7, pp. 9–15, Jun. 2017, doi: 10.5120/ijca2017914416.
- [23] H. Aboub, R. Mechouma, B. Azoui, C. Labiod, and A. Khechekhouch, "A new multicarrier sinusoidal pulse width modulation (SPWM) strategy based on rooted tree optimization (RTO) algorithm for reducing total harmonic distortion (THD) of switched-capacitor nine-level inverter in grid-connected PV systems," *Indonesian Journal of Science and Technology*, vol. 7, no. 1, pp. 19–36, Dec. 2021, doi: 10.17509/ijost.v7i1.41716.
- [24] N. A. Rahim and J. Selvaraj, "Multistring five-level inverter with novel PWM control scheme for PV application," *IEEE Transactions on Industrial Electronics*, vol. 57, no. 6, pp. 2111–2123, Jun. 2010, doi: 10.1109/TIE.2009.2034683.
- [25] B. N'Hili, A. Mesbahi, A. Nouaiti, M. K. Allah, S. Barakat, and A. Arif, "A new three-phase, five-level inverter with output voltage boost using a novel sinusoidal pulse width modulation," in *2023 3rd International Conference on Innovative Research in Applied Science, Engineering and Technology (IRASET)*, IEEE, May 2023, pp. 1–6. doi: 10.1109/IRASET57153.2023.10153048.
- [26] T. Windisch and W. Hofmann, "Loss minimizing and saturation dependent control of induction machines in vehicle applications," in *IECON 2015 - 41st Annual Conference of the IEEE Industrial Electronics Society*, IEEE, Nov. 2015, pp. 001530–001535. doi: 10.1109/IECON.2015.7392318.
- [27] B. H. Dinh and C. D. Tran, "Improved scalar control based on slip compensation from virtual speeds in three-phase induction motor drives," *International Journal of Power Electronics and Drive Systems (IJPEDS)*, vol. 15, no. 3, p. 1410, Sep. 2024, doi: 10.11591/ijpeds.v15.i3.pp1410-1416.

APPENDIX

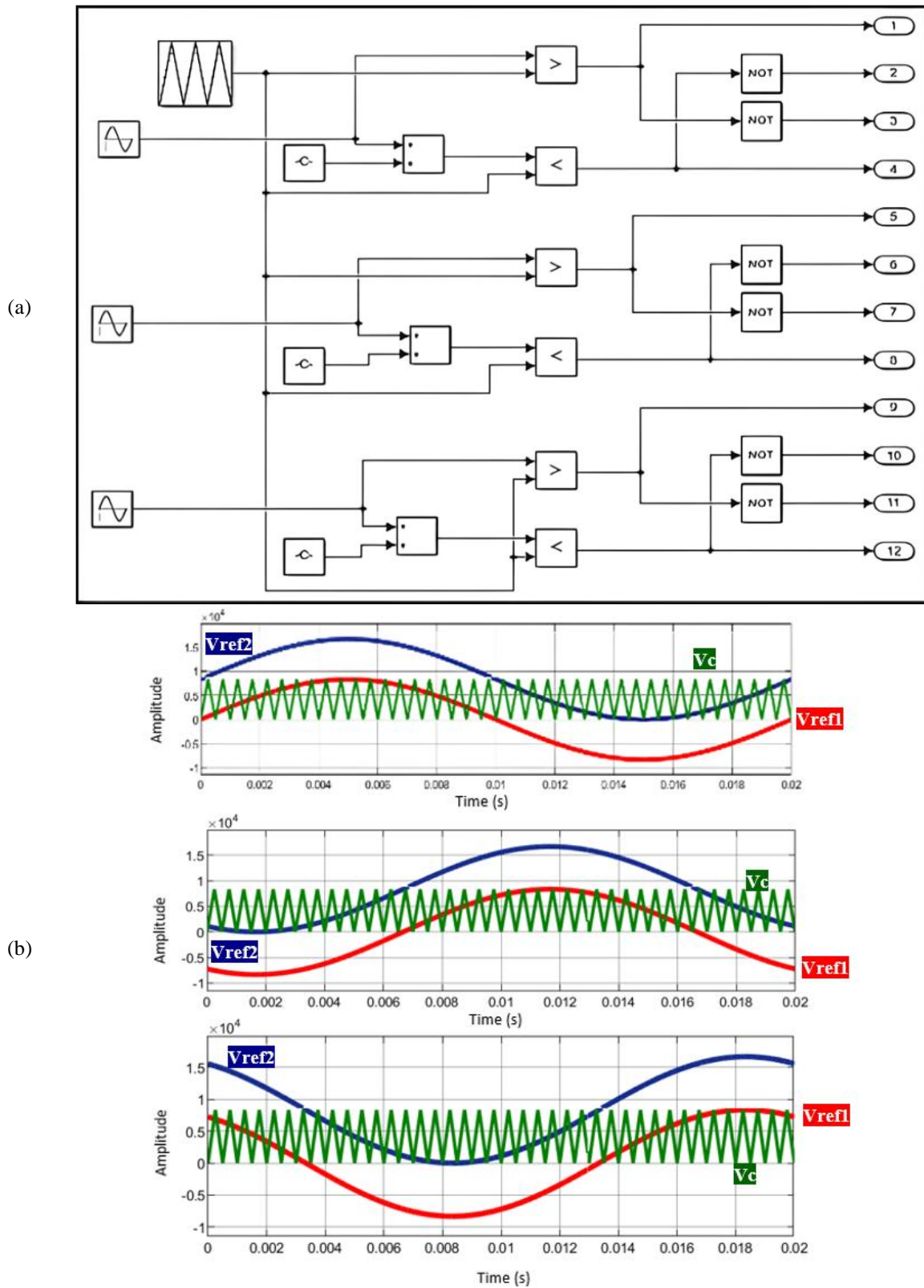










Figure 2. The proposed sinusoidal PWM technique: (a) the developed sinusoidal PWM algorithm and (b) the obtained carrier and reference signals are used for the switching pattern generation

BIOGRAPHIES OF AUTHORS







Badr N'hili     was born in Morocco in 1987. He is an electrical engineer who graduated from the National High School of Electricity and Mechanics (ENSEM), Casablanca, Morocco in 2020. He obtained his Master's degree in Automated Systems Engineering from the École Centrale de Lyon, France, in 2021. During 2020-2021, he was part of the engineering team at General Electric's wind turbine manufacturing plant in Saint-Nazaire, France. He is currently the Head of the Automotive Engineering Department at the Royal School of Materiel in Benslimane, Morocco. His research interests include electrical and electronic engineering, machine design, system modeling, control techniques, optimization, fault diagnosis, as well as wind turbine and solar energy technologies. He can be contacted at email: badr.nhili@ensem.ac.ma.







Souhail Barakat     is an electrical engineer since 2015, graduating from the Faculty of Sciences and Technology at Hassan II University Mohammedia, Morocco. He received an aggregate diploma degree in electrical engineering in 2019. Currently, he is a Ph.D. student in the Energy and Electrical Systems Laboratory (LESE) located in the National High School of Electricity and Mechanics (ENSEM) University Hassan 2, Casablanca, Morocco. His research focuses on renewable energies, control of power converters, intelligent algorithms, and energy quality. He can be contacted at email: souhail.barakat.doc21@ensem.ac.ma.







Abdelouahed Mesbahi     received the M.A. degree from ENSET, Rabat, Morocco, in 1990 and the DEA diploma in information processing in 1997 from Hassan II University, Faculty of Sciences, Ben M'sik, Casablanca, Morocco. He obtained the Ph.D. degree in engineering sciences from ENSEM Casablanca, Morocco, in 2013. Until 2013, he was a teacher in the Electrical Engineering Department at ENSET Mohammedia, Morocco. Actually, he serves as an assistant professor in the Electrical Engineering Department at ENSEM, Casablanca, Morocco. His research in the Energy and Electrical Systems Laboratory (LESE) is focused on sensorless control and advanced command applied to electrical machines and control of renewable energy systems. He is also an associated research member of the SSDIA Laboratory based in ENSET, Mohammedia, Morocco. He can be contacted at email: a.mesbahi@ensem.ac.ma.



Mohamed Khafallah     was born in Morocco in 1964. He received B.Sc., M.Sc., and Doctorate degrees from Hassan II University, Casablanca, in 1989, 1991, and 1995, respectively, all in Electrical Engineering. In 1995, he joined the National High School of Electricity and Mechanics (ENSEM), Hassan II University, Casablanca, Morocco, where he is currently a professor and tutor in the Department of Electrical Engineering and chief of the Laboratory of Energy and Electrical Systems (LESE). His main research interests are the application of power electronics converts and motor drives. He has published a lot of research papers in international journals, conference proceedings, as well as chapters of books. He can be contacted at email: m.khafallah@gmail.com.



Ayoub Nouaiti     is currently a qualified lecturer in the Department of Electrical Engineering at the Higher School of Technology (EST), Moulay Ismail University of Meknes, Morocco. He received his engineering degree in electrical engineering in 2011 and his Ph.D. in electrical engineering in 2019. His current research interests include the application of power electronics converters, motor drives, intelligent and digital control using DSP implementations, and renewable energy integration. He can be contacted at emails: nouayoub@gmail.com or a.nouaiti@umi.ac.ma.